JOURNAL OF PETROLEUM GEOMECHANICS
(JPG)

Experimental Study on the Impact of Joint Geometry on the Confined Compressive Strength of Jointed Rock Masses

Hadi Mokhtarian[1], Majid Noorian-Bidgoli[2]*, Hassan Moomivand[3]

1. PhD student of Mining Engineering, Engineering Department, University of Kashan, Kashan, Iran
2. Assistant Professor, Division of Mining Engineering, Engineering Department, University of Kashan, Kashan, Iran
3. Professor, Division of Mining Engineering, Engineering Department, Urmia University, Urmia, Iran

Received: 13 August 2024; Accepted: 16 November 2024

DOI: 10.22107/jpg.2025.472880.1239

Keywords

Compressive Strength, Failure, Joint roughness, Joint orientation, Joint filler, Confining pressure.

Abstract

In this article, the aim is to investigate the role of joint geometrical characteristics, including orientation, filler thickness, and roughness type, on the confined compressive strength of jointed rock masses. To achieve this, a series of comprehensive laboratory experiments was designed and conducted. In the first stage, limestone rock samples were used according to the experimental design. Using a cutting machine, two groups of samples were prepared with wavy and ribbed artificial roughness's at different angles of 0, 30, 45, and 60 degrees. To examine the effect of filler material thickness, gypsum and cement filler materials with specific resistances in thicknesses of 3, 5, and 8 mm were utilized. After triaxial laboratory tests were performed with a hook cell device at two confining pressure levels (5 and 14 MPa), the following key results were obtained: (a) higher confining pressures (14 MPa) significantly enhance compressive strength, with ribbed joints showing a more pronounced response than wavy joints, (b) for both roughness types, compressive strength was lowest at a 30-degree angle, highest at a 0-degree angle, and intermediate at a 60-degree angle, confirming the effect of anisotropy, and (c) thicker fillers generally improved strength at lower pressures but were less effective at higher pressures. These findings emphasize the importance of considering pressure conditions, joint orientation, and filler thickness in optimizing the mechanical behavior of jointed rock masses.

1. Introduction

The overall strength of rock masses is profoundly influenced by discontinuities, which are crucial in determining the mechanical properties and strength reduction of rocks. Understanding the shear strength of these discontinuities is essential due to their significant impact on rock stability, particularly in engineering applications such as mining, tunneling, and slope stability. Previous studies have predominantly employed direct shear tests to investigate these properties, revealing the inherent complexity in characterizing shear resistance and other attributes of rock joints. Research into the shear strength of rock discontinuities has provided valuable insights through tests conducted under two primary boundary conditions: constant normal load/stress (CNL) and constant normal stiffness (CNS). In CNL conditions, where normal stress remains constant, joint surfaces can freely dilate during shearing [1]. Conversely, CNS conditions restrict joint dilation, resulting in higher peak shear strength, friction angle, and cohesive strength values [2]. Consequently, CNS tests offer a more comprehensive representation of rock joint roughness compared to CNL tests. However, replicating the complexity of these conditions in testing jointed specimens under triaxial

* **Corresponding Author:** noriyan@kashanu.ac.ir

compressive stresses presents significant challenges.

Recent research has further explored the influence of natural infill materials on discontinuity strength parameters. For instance, Jahanian and Sadaghiani [3] investigated the shear strength of sandy clay-infilled saw-tooth rough joints, highlighting the limited impact of infill thickness compared to surface roughness and asperity inclination, even under higher normal stress levels. Similarly, Karakus et al. [4] studied the effect of infill thickness on joint compressive strength (JCS) and overall shear strength, noting minimal variations in JCS up to a threshold infill thickness of 2 mm. Their work led to the development of a novel shear strength model for rock joints that integrates infill thicknesses ranging from 1 to 6 mm. Furthermore, studies have delved into the impact of discontinuity orientation on unfilled jointed rock strength under triaxial stresses, focusing on evaluating rock failure criteria parameters based on unfilled jointed specimens. Sinha and Singh's [5] research on cylindrical plastic specimens with undulating and planar discontinuity surfaces underscored the significant influence of infill material on specimen strength and mechanical behavior. Mokhtarian et al. [6] examined the influence of infilled discontinuities on rock failure mechanisms under triaxial stresses, creating various types of infilled discontinuities using different infill materials with varying compositions and uniaxial compressive strengths. Their findings highlighted the substantial impact of infill material composition and orientation angle on jointed rock failure criteria parameters.

Moreover, Xu et al. [7] investigated the profound impact of stiff discontinuities on deep hard rock engineering disasters through true triaxial tests on marble samples. They analyzed the influence of discontinuity inclination angles, thicknesses, and stress states on deformation and failure mechanisms during excavation. The experimental results demonstrated that post-peak deformation and failure characteristics are significantly affected by these factors. Similarly, Wu et al. [8] focused on the shear strength deterioration of bedding planes between different rock types induced by cyclic loading, aiming to evaluate the stability of interbedded bedding rock slopes under earthquake conditions.

Despite these advancements, gaps persist in our understanding of how infill material properties influence discontinuities with varying orientations on failure mechanisms and jointed rock failure criteria parameters under triaxial compressive stresses. This study seeks to bridge this gap by identifying the effect of infill material properties on jointed rock failure criteria parameters under triaxial compressive stresses.

Numerous scholars have explored the mechanical behavior of jointed rock masses through numerical simulation. Vergara et al. [9] used UDEC to study the strength and failure modes of rock containing non-persistent joints, finding that joint spacing and angle significantly influence the uniaxial strength of the rock. Bahaaddin et al. [10] employed PFC 3D to analyze the effects of joint geometrical parameters, including joint orientation angle, spacing, persistency degree, step angle, and aperture on UCS and the deformation modulus, concluding that joint orientation angle had the greatest effects on the mechanical characteristics of rock masses.

In addition to numerical simulations, the influence of joint geometrical specifics on the failure criteria of jointed rock masses has been extensively researched. Yang et al. [11] conducted biaxial compression tests on rock-like specimens with non-persistent joints, emphasizing the significant impact of joint geometry, principal stress orientation, and intact material compressive strength on the failure modes and strengths of jointed rock masses. Similarly, Liu et al. [12] explored the effects of joint set numbers and joint geometry configuration on the failure mode, unconfined compressive strength, and Young’s modulus of jointed rock masses. Han et al. [13] investigated the influence of joint dip angle on the mechanical behavior of infilled jointed rock masses under different compression conditions. Moreover, Li et al. [14] analyzed various joint geometrical parameters such as orientation angle, spacing, persistency degree, step angle, and aperture, and their effects on the unconfined compressive strength and deformation modulus of rock masses, concluding that these parameters significantly impact the mechanical characteristics of rock masses. Additionally, Li et al. [14] developed linear and nonlinear failure criteria for rock masses with non-penetrating joints, highlighting the importance of joint strength and shear strength in determining the overall strength of the rock mass.

The primary objective of this study is to

experimentally investigate the impact of joint geometrical specifics, including orientation angle, spacing, persistency degree, step angle, and aperture, on the confined compressive strength and failure mechanisms of jointed rock masses. By using physical modeling and incorporating infill materials with varying uniaxial compressive strengths (UCS), this research aims to provide a comprehensive understanding of how these geometrical characteristics interact under triaxial stress conditions. The findings will contribute to the development of more accurate predictive models and enhance safety measures in rock engineering applications. This study innovatively combines the hook cell test under CNL conditions with an evaluation of the filler material thickness, thereby advancing the understanding of jointed rock mass behavior under complex stress states. By integrating these methods, we aim to provide deeper insights into the interplay between infill material properties and rock joint mechanical behavior, ultimately contributing to more accurate predictive models and safer engineering practices in rock mechanics.

2. Methodology

In this article, the aim is to investigate the role of joint geometrical characteristics on the confined compressive strength of the jointed rock mass. To achieve this, as outlined in the flowchart in Figure 1, a series of comprehensive laboratory tests were conducted to study the effect of directional characteristics, filler thickness, and roughness type on the confined resistance of jointed rock under triaxial loading using a Hook cell. The research followed a systematic approach involving several key stages:

First, the experiment design was meticulously planned. In the second stage, cores were extracted and prepared from a limestone sample. In the third step, a cutting machine was used to create two sets of cores with artificial roughness, specifically wavy (W-type) and ridged (S-type), at different angles of 0, 30, 45, and 60 degrees. The fourth step involved investigating the effect of filler material thickness by using plaster and cement fillers with specific resistances at thicknesses of 3, 5, and 8 mm. In the fifth step, triaxial testing was performed with a Hook cell under two confining pressures of 5 and 14 MPa. Finally, the sixth step entailed analyzing the results from the laboratory tests on 48 jointed core samples. This systematic approach allowed for a detailed examination of how joint geometrical specifics, filler material properties, and roughness types influence the confined compressive strength of jointed rock masses under triaxial loading conditions.

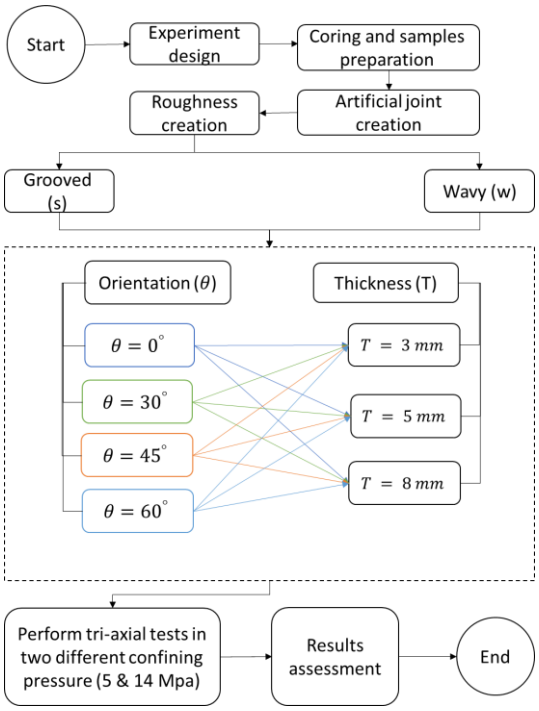

Figure 1. Flowchart implemented in this research

3. Results and Conclusions

3.1. Sample preparing

To replicate natural materials, various combinations of plaster, sand, clay, and water were selected for their suitability in modeling infill materials within discontinuity apertures. Three types of infill materials (F1, F2, and F3) were formulated based on these combinations, as detailed in Table 1. The grain size distribution of the sand used in these mixtures is outlined in Table 2. Cylindrical specimens were then created using the mortar derived from these infill materials. Before testing, the fracture surfaces of these specimens were shaped into grooved or wavy patterns using a CNC tool, as shown in Figure 2. The specimens were subjected to uniaxial compressive strength (UCS) testing after drying, following the standard procedure [15]. The UCS results, along with the friction angle (φ_j) and adhesion strength (C_j) for each type of infill material, are presented in Table 3. A direct

shear test was conducted according to standard [16] to determine the friction angle (φj) and adhesion strength (Cj) of these filled discontinuities. It was found that in the absence of sand in the infill material, the specimens exhibited characteristics more similar to the natural rock mass. Therefore, F2 material was chosen for the fill of the aperture.

Table 1. The weight proportions of the constituent components in the infill materials within the discontinuity apertures

Infill materials	Weight percentage of the constituent components relative to the total weight of water, plaster, clay, and sand			
	Clay (%)	Sand (%)	Plaster (%)	Water (%)
F1	16.66	33.33	16.66	33.33
F2	25	0	37.5	37.5
F3	0	40	30	30

Table 2. The weight distribution of granulation in the sand used for the infill materials within the discontinuity apertures

No.	Granulation	Passed weight percentage
1	2.36 mm sieve	100
2	1.18 mm sieve	90
3	0.6 mm sieve	46.2
4	0.3 mm sieve	17.5
5	0.15 mm sieve	4.3

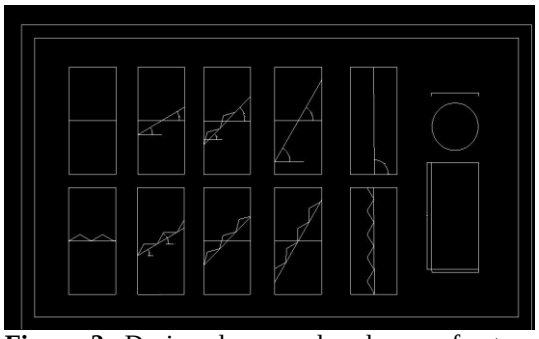

Figure 2. Designed grooved and wavy fracture surfaces for samples in different orientation

To assess the impact of infill materials on the failure behavior of discontinuities at different orientations under triaxial stress, cylindrical limestone specimens were prepared following the standard (Figure 3). These specimens featured discontinuities at angles of 0°, 30°, 45°, 60°, and 90° relative to the horizontal. The prepared mortar was then placed in the apertures of these discontinuities. Five different sections of limestone were cut using a diamond saw, with each section containing discontinuities at angles of 0°, 30°, 45°, 60°, and 90°. The apertures in each section were filled with one of the three infill materials, with strengths of 0.616, 2.203, and 3.920 MPa, and thicknesses of 3 mm, 5 mm, or 8 mm, as shown in Figures 2 and 3. After drying, the specimens' strength was measured through triaxial compression tests under confining pressures of 5 MPa and 14 MPa, in accordance with standards [15–17]. Previous research indicates that the shape, size, and roughness of the wall surface do not significantly affect adhesion strength and friction angle since the discontinuity walls do not come into contact when filled [10,18,19].

Figure 3. Some of the prepared rock samples in order to conduct confined compressive test

Table 3. The UCS in the model materials, along with the friction angle (φ_j) and adhesion strength (C_j) in three types of model infill materials within the discontinuity aperture.

Infill material	Average UCS (MPa)	Adhesion strength (C) of discontinuity filled with model material (MPa)	Friction angle (ϕ) of discontinuity filled with model material (degree)
F1	0.616	0.106	43.52
F2	2.203	0.278	38.9
F3	3.930	0.170	52.43

Sample No. of	Thickness (mm)	Joint Type	θ (°)	σ_3 MPa	σ_1 MPa	Sample No. of	Thickness (mm)	Joint Type	θ (°)	σ_3 MPa	σ_1 MPa
1	8	w	0	5	38.28	**25**	8	w	0	14	95.09
2			30	5	20.61	**26**			30	14	73.6
3			45	5	19.35	**27**			45	14	52.79
4			60	5	34.8	**28**			60	14	58.22
5		S	0	5	29.12	**29**		S	0	14	113.53
6			30	5	34	**30**			30	14	76.41
7			45	5	31.6	**31**			45	14	72.26
8			60	5	28.72	**32**			60	14	58.6
9	5	w	0	5	28.45	**33**	5	w	0	14	72
10			30	5	33.59	**34**			30	14	71.88
11			45	5	40.13	**35**			45	14	46.31
12			60	5	41.98	**36**			60	14	60.99
13		S	0	5	35.85	**37**		S	0	14	69.87
14			30	5	35.49	**38**			30	14	68.03
15			45	5	32.81	**39**			45	14	72.3
16			60	5	32.23	**40**			60	14	54.75
17	3	w	0	5	37.83	**41**	3	w	0	14	77.64
18			30	5	46.83	**42**			30	14	68.15
19			45	5	39.54	**43**			45	14	56.18
20			60	5	24.51	**44**			60	14	61.34
21		S	0	5	38.59	**45**		S	0	14	81.45
22			30	5	25.35	**46**			30	14	47.65
23			45	5	37.58	**47**			45	14	74.27
24			60	5	29.09	**48**			60	14	68

3.2. Test conduction

In the triaxial test using a Hoek cell, each cylindrical specimen, containing a discontinuity at a specific orientation, is first placed inside a rubber membrane that is securely sealed to prevent any fluid intrusion during testing. This membrane-enclosed specimen is then positioned within the Hoek cell, which is subsequently filled with hydraulic fluid to apply the required confining pressure. Once the confining pressure is uniformly applied, creating isotropic stress around the specimen, an axial load is gradually introduced through a loading piston that extends through the top of the Hoek cell. This process simulates triaxial stress conditions while maintaining the constant confining pressure. During the test, as the axial load increases, the specimen undergoes deformation, with both axial and radial strains being continuously recorded by sensors. The test continues until the specimen fails, either by fracturing or sliding along the filled discontinuity. The peak stress observed at failure represents the triaxial compressive strength of the specimen under the specified confining pressure, and these results are presented in Table 4.

3.3. Analyzing the Impact of Joint Geometric Properties

3.3.1. Joint roughness

Figure 4 presents the variations in confined compressive strength of rock samples with W-type and S-type joint surfaces, across different confining pressures and filler thicknesses. As can be seen, the confined compressive strength of jointed rock masses is significantly influenced by confining pressure, joint angle, and filler thickness. Higher confining pressures (14 MPa) generally result in increased compressive

strengths across all angles and filler thicknesses, with W-type samples showing a more pronounced response compared to S-type samples. As the joint angle increases, W-type samples tend to exhibit a decrease in strength, particularly under higher confining pressure, whereas S-type samples demonstrate less variation in strength at 5 MPa but show significant fluctuations at 14 MPa. Regarding filler thickness, samples with 3 mm and 5 mm thicknesses typically exhibit higher strengths compared to those with 8 mm thickness, which generally show lower strengths, especially at higher angles (30°, 45°, 60°). When comparing W-type and S-type joints, W-type samples often exhibit higher strengths at smaller angles (0°, 30°) under high confining pressure but lower strengths at larger angles (45°, 60°), while S-type samples display more consistent strength values across different angles and confining pressures, with notably high strength at 14 MPa and lower angles. This highlights the complex interplay of joint geometrical specifics, roughness type, angle, and filler thickness on the mechanical behavior of jointed rock masses under confined compressive conditions.

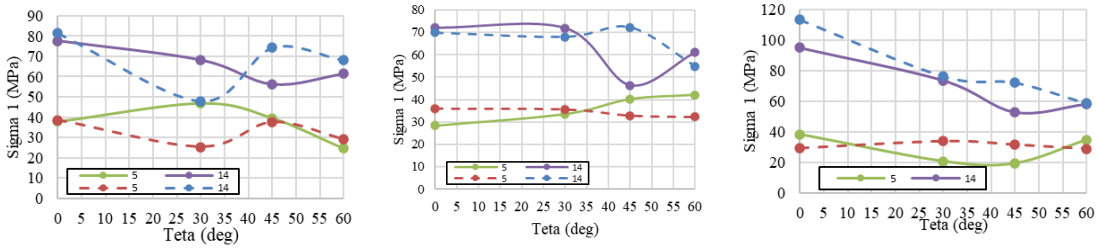

Figure 4. Confined compressive strength of W-type and S-type jointed samples at different angles and confining pressures; a) thickness 3 mm, b) thickness 5 mm, c) thickness 8 mm.

3.3.2. Joint orientation

Figure 5 depicts the variations in confined compressive strength of rock samples with different filling thicknesses for both W-type and S-type joint surfaces under a confining pressure of 5 MPa. The confined compressive strength of jointed rock samples is influenced by joint angles, filler thicknesses, and the type of joint (W-type and S-type), as observed under a confining pressure of 5 MPa. For W-type joints, the compressive strength values at different angles (0°, 30°, 45°, and 60°) show considerable variation with the change in filler thickness. At a thickness of 3 mm, the compressive strength starts high at 37.83 MPa at 0°, increases to 46.83 MPa at 30°, slightly decreases to 39.54 MPa at 45°, and drops to 24.51 MPa at 60°. With a 5 mm thickness, the strength begins at 28.45 MPa at 0°, increases consistently through the angles, peaking at 41.98 MPa at 60°. At an 8 mm thickness, the compressive strength is 38.28 MPa at 0°, decreases to 20.61 MPa at 30° and 19.35 MPa at 45°, and then increases to 34.80 MPa at 60°. For S-type joints, the compressive strength also varies with joint angles and filler thicknesses. At a 3 mm thickness, the strength is 38.59 MPa at 0°, drops significantly to 25.35 MPa at 30°, rises to 37.58 MPa at 45°, and decreases again to 29.09 MPa at 60°. At a 5 mm thickness, the strength begins at 35.85 MPa at 0°, remains relatively stable around 35 MPa at 30°, drops slightly to 32.81 MPa at 45°, and ends at 32.23 MPa at 60°. With an 8 mm thickness, the strength starts at 29.12 MPa at 0°, peaks at 34 MPa at 30°, decreases to 31.60 MPa at 45°, and further decreases to 28.72 MPa at 60°. Figure 6 illustrates how the confined compressive strength of rock samples changes with varying filler thicknesses for W-type and S-type joint surfaces under a confining pressure of 14 MPa. Under a confining pressure of 14 MPa, the confined compressive strength of jointed rock samples exhibits distinct trends based on joint angles, filler thicknesses, and joint types. For W-type joints, at a filler thickness of 3 mm, the compressive strength starts at 81.45 MPa at a 0° joint angle, drops to 47.65 MPa at 30°, increases to 74.27 MPa at 45°, and then rises again to 68 MPa at 60°. At a thickness of 5 mm, the compressive strength begins at 69.87 MPa at 0°, remains relatively stable at 68.03 MPa at 30°, peaks at 72.3 MPa at 45°, and drops to 54.75 MPa at 60°. With an 8 mm thickness, the strength is highest at 113.53 MPa at 0°, decreases

significantly to 76.41 MPa at 30°, further drops to 72.26 MPa at 45°, and reaches the lowest value of 58.6 MPa at 60°. For S-type joints, at a 3 mm thickness, the compressive strength starts at 77.64 MPa at 0°, decreases to 68.15 MPa at 30°, drops further to 56.18 MPa at 45°, and slightly increases to 61.34 MPa at 60°. At a 5 mm thickness, the strength is 72 MPa at 0°, remains consistent at 71.88 MPa at 30°, drops sharply to 46.31 MPa at 45°, and increases to 60.99 MPa at 60°. At an 8 mm thickness, the compressive strength is 95.09 MPa at 0°, decreases steadily to 73.6 MPa at 30°, drops further to 52.79 MPa at 45°, and slightly rises to 58.22 MPa at 60°.

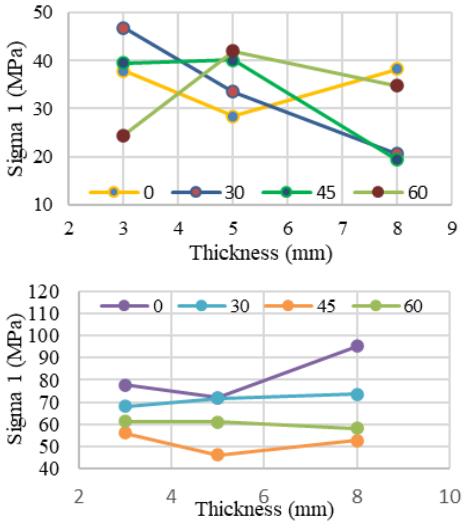

Figure 5. Confined compressive strength of rocksamples with W-type joints in different thicknesses; a) confined pressure 5 MPa, b) confined pressure 14 MPa

Comparing the results under confining pressures of 5 MPa and 14 MPa reveals notable differences in compressive strengths. At 5 MPa, W-type joints generally show higher compressive strengths at lower joint angles (0°, 30°), with significant variations at higher angles (45°, 60°). In contrast, at 14 MPa, W-type joints exhibit a pronounced increase in compressive strength, particularly at the 0° angle with an 8 mm filler, highlighting the substantial impact of increased confining pressure. S-type joints, under 5 MPa, show consistent strength across different angles, with significant strength at 3 mm filler and 45° angle. Under 14 MPa, S-type joints display a similar pattern of strength variation, but with generally higher values across all angles and filler thicknesses. The increased confining pressure of 14 MPa significantly enhances the compressive strengths of both W-type and S-type joints, with W-type joints showing a more pronounced increase, especially at smaller angles and thicker fillers. This demonstrates that higher confining pressures can substantially improve the mechanical behavior of jointed rock masses, emphasizing the importance of considering pressure conditions in rock engineering applications.

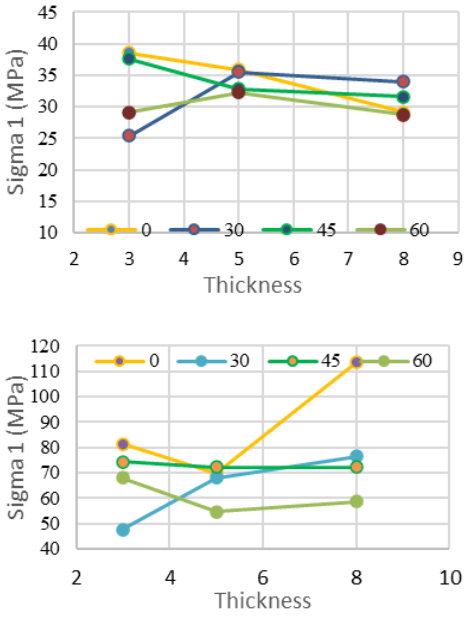

Figure 6. Confined compressive strength of rock samples with S-type joints in different thicknesses; a) confined pressure 5 MPa, b) confined pressure 14 M

4. Conclusion

In this study, the objective was to examine the impact of joint geometrical characteristics namely orientation, filler thickness, and roughness type on the confined compressive strength of jointed rock masses. A series of detailed laboratory experiments were carried out. Initially, limestone rock samples were prepared according to the experimental design. Two groups of samples were created using a cutting machine, introducing artificial roughnesses classified as wavy and ribbed at angles of 0°, 30°, 45°, and 60°. To analyze the effect of filler material thickness, gypsum and cement fillers with specific resistances were applied in thicknesses of 3 mm, 5 mm, and 8 mm. Triaxial laboratory tests were then conducted using a hook cell device at two different confining pressure levels: 5 MPa and 14

MPa. The study reveals significant trends in the confined compressive strength of jointed rock masses influenced by confining pressure, joint roughness, joint orientation, and filler thickness:
Higher confining pressures (14 MPa) generally result in increased compressive strengths across all joint angles and filler thicknesses.
W-type joints show a more pronounced response to higher confining pressure compared to S-type joints.
At 14 MPa, both W-type and S-type joints demonstrate higher compressive strengths than at 5 MPa, emphasizing the substantial impact of increased confining pressure on rock strength.
W-type joints typically exhibit higher compressive strengths at smaller joint angles (0°, 30°) under high confining pressure but lower strengths at larger angles (45°, 60°).
S-type joints display more consistent strength values across different angles and confining pressures, with particularly high strength at 14 MPa and lower angles.
W-type joints show significant variation in compressive strength with joint angles, particularly under higher confining pressure. Strength generally decreases with increasing joint angle under 14 MPa.
S-type joints exhibit less variation in strength at 5 MPa but show significant fluctuations at 14 MPa.
Generally, samples with 3 mm and 5 mm filler thicknesses exhibit higher compressive strengths compared to those with 8 mm thickness.
Thicker fillers tend to show higher initial compressive strengths but may vary more significantly with joint angles.
At lower confining pressures (5 MPa), thicker fillers contribute positively to strength at certain orientations (0° and 45°), whereas other orientations (60°) exhibit less consistent changes.
At higher confining pressures (14 MPa), the overall compressive strength generally decreases across most orientations and thicknesses, indicating that higher pressures may diminish the positive impact of filler thickness on strength.

5. References

[1] Poturovic, W. Schubert, M. Blümel S, Comparison of constant normal load (CNL) and constant normal stiffness (CNS) direct shear tests, in: ISRM EUROCK, ISRM, 2015: p. ISRM-EUROCK.

[2] S. Thirukumaran, B. Indraratna, A review of shear strength models for rock joints subjected to constant normal stiffness, J. Rock Mech. Geotech. Eng. 8 (2016) 405–414.

[3] H. Jahanian, M.H. Sadaghiani, Experimental study on the shear strength of sandy clay infilled regular rough rock joints, Rock Mech. Rock Eng. 48 (2015) 907–922.

[4] M. Karakus, Y. Liu, G. Zhang, H. Tang, A new shear strength model incorporating influence of infill materials for rock joints, Geomech. Geophys. Geo-Energy Geo-Resources. 2 (2016) 183–193.

[5] U.N. Sinha, B. Singh, Testing of rock joints filled with gouge using a triaxial apparatus, Int. J. Rock Mech. Min. Sci. 37 (2000) 963–981.

[6] H. Mokhtarian, H. Moomivand, H. Moomivand, Effect of infill material of discontinuities on the failure criterion of rock under triaxial compressive stresses, Theor. Appl. Fract. Mech. 108 (2020) 102652.

[7] H. Xu, Z. Zhang, Y.-J. Zhang, Q. Jiang, S.-L. Qiu, Y.-Y. Zhou, G.-L. Feng, Effects of natural stiff discontinuities on the deformation and failure mechanisms of deep hard rock under true triaxial conditions, Eng. Fail. Anal. 158 (2024) 108034.

[8] Q. Wu, Z. Liu, H. Tang, L. Wang, X. Huo, Z. Cui, S. Li, B. Zhang, Z. Lin, Experimental investigation on shear strength deterioration at the interface between different rock types under cyclic loading, J. Rock Mech. Geotech. Eng. (2024).

[9] M.R. Vergara, M. Van Sint Jan, L. Lorig, Numerical model for the study of the strength and failure modes of rock containing non-persistent joints, Rock Mech. Rock Eng. 49 (2016) 1211–1226.

[10] M. Bahaaddini, P. Hagan, R. Mitra, B.K. Hebblewhite, Numerical study of the mechanical behavior of nonpersistent jointed rock masses, Int. J. Geomech. 16 (2016) 4015035.

[11] W. Yang, G. Li, P.G. Ranjith, L. Fang, An experimental study of mechanical behavior of brittle rock-like specimens with multi-non-persistent joints under uniaxial compression and damage analysis, Int. J. Damage Mech. 28 (2019) 1490–1522.

[12] J. Liu, S. Sun, L. Yue, J. Wei, J. Wu, Mechanical and failure characteristics of rock-like

material with multiple crossed joint sets under uniaxial compression, Adv. Mech. Eng. 9 (2017) 1687814017708710.

[13] G. Han, H. Jing, Y. Jiang, R. Liu, H. Su, J. Wu, The effect of joint dip angle on the mechanical behavior of infilled jointed rock masses under uniaxial and biaxial compressions, Processes. 6 (2018) 49.

[14] B. Li, Y. Jiang, T. Mizokami, K. Ikusada, Y. Mitani, Anisotropic shear behavior of closely jointed rock masses, Int. J. Rock Mech. Min. Sci. 71 (2014) 258–271.

[15] ASTM, Unconfined compressive strength of intact rock core, ASM Annual Book of Standards, D2938-36, 1994.

[16] ASTM, Standard test method for triaxial compressive strength of undrained rock core specimens without pore pressure measurements, ASTM Annual Book of Standards, D2664 – 95a, 1997.

[17] R.I. Annually, ASTM STANDARDS, (1995).

[18] S.A. Gulmus, U. Yilmazer, Effect of the surface roughness and construction material on wall slip in the flow of concentrated suspensions, J. Appl. Polym. Sci. 103 (2007) 3341–3347.

[19] N. Barton, C. Wang, R. Yong, Advances in joint roughness coefficient (JRC) and its engineering applications, J. Rock Mech. Geotech. Eng. 15 (2023) 3352–3379.